



**HAL**  
open science

## **Ultracompact reference ultralow expansion glass cavity**

Alexandre Didier, Jacques Millo, Baptiste Maréchal, Cyrus Rocher, Enrico Rubiola, Roméo Lecomte, Morvan Ouisse, Jérôme Delporte, Clément Lacroute, Yann Kersalé

### ► To cite this version:

Alexandre Didier, Jacques Millo, Baptiste Maréchal, Cyrus Rocher, Enrico Rubiola, et al.. Ultracompact reference ultralow expansion glass cavity. *Applied optics*, 2018, 57 (22), pp.6470-6473. <10.1364/AO.57.006470>. <hal-02138795>

**HAL Id: hal-02138795**

**<https://hal.science/hal-02138795v1>**

Submitted on 23 Oct 2019

**HAL** is a multi-disciplinary open access archive for the deposit and dissemination of scientific research documents, whether they are published or not. The documents may come from teaching and research institutions in France or abroad, or from public or private research centers.

L'archive ouverte pluridisciplinaire **HAL**, est destinée au dépôt et à la diffusion de documents scientifiques de niveau recherche, publiés ou non, émanant des établissements d'enseignement et de recherche français ou étrangers, des laboratoires publics ou privés.



HAL Authorization

# Ultracompact reference ultralow expansion glass cavity

ALEXANDRE DIDIER,<sup>1,2</sup> JACQUES MILLO,<sup>1</sup> BAPTISTE MARECHAL,<sup>1</sup> CYRUS ROCHER,<sup>1</sup> ENRICO RUBIOLA,<sup>1</sup> ROMÉO LECOMTE,<sup>1</sup> MORVAN OUISSE,<sup>1</sup> JÉRÔME DELPORTE,<sup>3</sup> CLÉMENT LACROÛTE,<sup>1</sup>  AND YANN KERSALÉ<sup>1,\*</sup>

<sup>1</sup>FEMTO-ST Institute, Univ. Bourgogne Franche-Comté, CNRS, ENSMM, Besançon, France

<sup>2</sup>PTB, Bundesallee 100, 38116 Braunschweig, Germany

<sup>3</sup>Centre National d'Etudes Spatiales (CNES), Toulouse, France

\*Corresponding author: yann.kersale@femto-st.fr

We present the first experimental characterization of our ultracompact, ultrastable laser. The heart of the apparatus is an original Fabry Perot cavity with 25 mm length and pyramidal geometry, equipped with highly reflective crystalline coatings. The cavity, along with its vacuum chamber and optical setup, fits inside a 30 L volume. We have measured the cavity's thermal and vibration sensitivities and present our first estimation of the cavity fractional frequency instability at  $\sigma_y(1s)=7.5 \times 10^{-15}$ .

## 1. INTRODUCTION

High-finesse Fabry–Perot cavities are widely used as frequency references to stabilize laser sources. The improvement of these cavity-stabilized lasers are of prime importance for optical frequency standards [1]. Consequently, many laboratories are developing techniques to reduce the thermal noise of cavities, which now reaches the  $10^{-17}$  decade, at the cost of complex systems such as cryocoolers [2,3] and active control of many technical parameters such as residual amplitude modulation, frequency fluctuations induced by the Doppler effect, or intensity fluctuations [4].

In addition, these highly stable lasers are also used to synchronize optical frequency combs for ultralow phase noise microwave signal generation [5–7], with ultralow frequency comb residual noise [7,8]. Precision spectroscopy is also a field of interest. Such applications do not require state-of-the-art stabilized lasers, but compactness and simplicity are important criteria [9]. For this purpose, we are developing a laser based on a 25 mm long cavity with a compact vacuum chamber and an optical setup reduced to the quintessential components.

In this paper, we present our ultracompact stabilized laser design and present our first measurement of thermal and vibration sensitivities as well as preliminary estimation of the stabilized laser phase noise and fractional frequency stability.

## 2. DESCRIPTION OF THE ULTRACOMPACT STABILIZED LASER SETUP

### A. Cavity Design

Several geometries have already been used to develop ultrastable Fabry–Perot cavities: horizontal and vertical cylinders and

spherical and cubic spacers. Here, we have developed a double tetrahedral geometry, which is a good compromise among length, volume, and thermal noise floor while keeping the overall cavity symmetry in order to reach low residual vibration sensitivity. Our cavity is 25 mm long, corresponding to a free spectral range of 6 GHz, with a total spacer height of 36 mm. The cavity fits in an overall volume of 35 mm  $\times$  36 mm  $\times$  41 mm (Fig. 1). More details on the cavity design and the finite element simulations can be found in [10].

The tetrahedral spacer is machined in ultra low expansion glass (ULE), while the cavity mirrors substrates are made of fused silicate. In order to reduce the coefficient of thermal expansion (CTE) zero-crossing shift due to the different CTE of ULE and fused silicate, ULE rings with dimensions of 12.7 mm outer diameter, 5 mm inner diameter, and 1 mm thickness have been contacted to back of the cavity mirrors in order to obtain a CTE zero crossing near 11°C [11].

The highly reflective coatings are made of crystalline GaAs/Al<sub>0.92</sub>Ga<sub>0.08</sub>As [12]. These coatings exhibit lower mechanical losses than those of traditional dielectric coatings, thus reducing the cavity thermal noise floor. In our case, the use of crystalline coatings leads to a theoretical thermal noise floor around  $1 \times 10^{-15}$ , which is remarkable for such a short cavity. The cavity finesse at 1542 nm has been determined using the ringdown method. The  $1/e$  decay time of the exponential fit is 6.56  $\mu$ s, yielding an optical finesse of 247,000 for a mirror radius of curvature of 240 mm. This is, to our knowledge, the highest published finesse for an ultrastable Fabry–Perot cavity based on crystalline coatings.

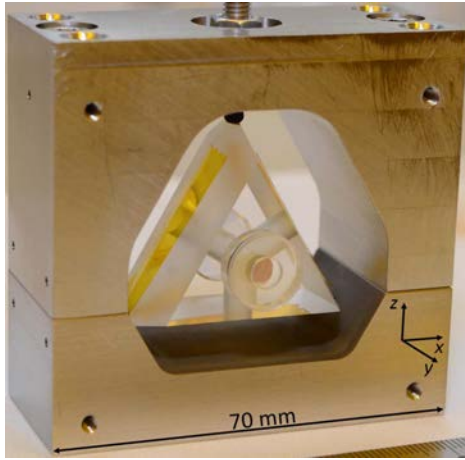


**Fig. 1.** Double tetrahedral cavity in its stainless-steel support. A Viton sphere on top of the cavity and two Viton pads at the bottom are used to fix the cavity in its support.

## B. Vacuum Chamber

In order to reduce the setup footprint, a custom cubic vacuum chamber was designed and assembled. It allows for direct mounting of free-space optical elements to its walls, where breadboards have been included (see Fig. 2). Thermal fluctuations are mitigated using a passive stainless-steel shield made with the cavity holder and surrounded by an additional active copper shield (see [10] for details). Thanks to its high density, stainless steel indeed offers a high thermal capacitance for a given volume. The active temperature control is made using a Peltier element placed under the copper shield; the resulting temperature stability of the copper shield is below  $2 \times 10^{-4}$  K

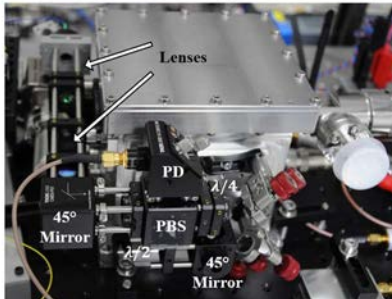
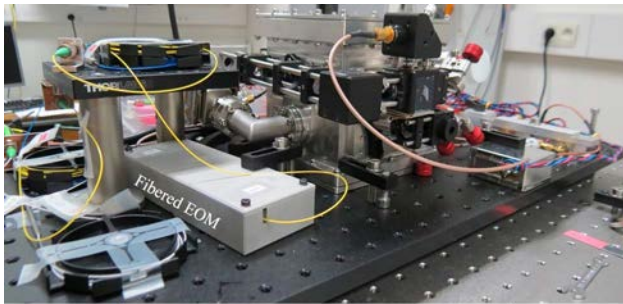


**Fig. 2.** Optical setup. Top: 30 cm  $\times$  60 cm breadboard, including the cavity in its vacuum chamber and all the optical setup except the laser source. Bottom: Close-up of the vacuum chamber with integrated optics for the light injection in the ultracompact ULE cavity. EOM, electro-optic modulator; PD, photodiode; PBS, polarized beam splitter.

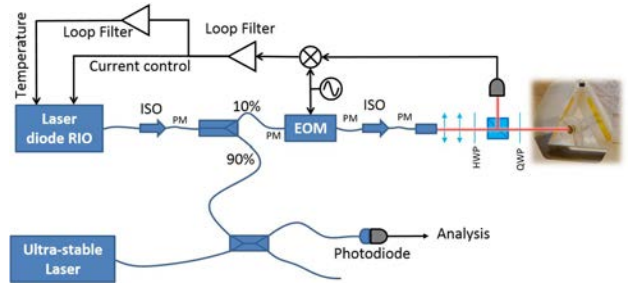


**Fig. 3.** Schematic of the laser stabilized on the ultracompact cavity. All the components are fiber pigtailed except for the cavity mode-matching. The free-space portion of the beam is represented in red in the graphic. HWP, half-wave plate; QWP, quarter-wave plate; PM, polarization maintaining; ISO, optical isolator.

between 1 s and  $4 \times 10^4$  s. The cavity response to a temperature step was fitted with a  $1/e$  response time of 20,000 s. The estimated attenuation of temperature fluctuations by the passive shield is around 100 dB at 1 Hz.

## C. Optical Setup

The optical setup has been boiled down to its quintessential elements. Only the mode-matching optics are free-space and based on 1/2-in. optical elements (see Fig. 3). The rest of the optical setup is based on pigtailed components with polarization-maintaining fiber for compactness. The laser source is a compact, fibered extended cavity diode laser (RIO Planex) at 1542 nm. Its is packaged in a pigtailed butterfly case that we integrated in a homemade electronic control rack, including a low-noise current source with an integrated current noise of 658 nA between 10 Hz and 100 kHz and a digital temperature controller. A 90/10 optical coupler is used to extract the ultrastable signal. A fibered electro-optic modulator (EOM) connected just before the output collimator provides phase modulation for the Pound–Drever–Hall stabilization method.

## 3. ULTRASTABLE LASER CHARACTERIZATION

### A. Vibration Sensitivities

Our simulations have predicted low acceleration sensitivities for the double-tetrahedral geometry of our spacer. We have developed a dedicated setup for a well-controlled measurement of accelerations. The ultrastable laser, including the vacuum chamber and the optical setup described in the previous section, is mounted on a thin aluminum breadboard supported by sorbothane posts. This apparatus is placed on an active vibration isolation platform, which can be modulated at frequencies between 0.1 Hz and 200 Hz in all directions. The platform is, in turn, placed on an optical table that provides passive isolation from ground vibrations.

The acceleration sensitivity coefficients  $k_{x,y,z}$  relate to the cavity fractional frequency noise  $S_y$  to the acceleration noise  $S_a$  so that

$$S_y = \sum_{i=x,y,z} k_i^2 S_{a_i},$$

where  $y$  is along the cavity optical axis,  $z$  is along the vertical direction, and  $x$  is along the remaining transverse direction.

**Table 1. Acceleration Sensitivities Along the  $x$ ,  $y$ , and  $z$  Measured at 2 and 6 Hz**

Direction	Measured at 2 Hz	Measured at 6 Hz
$x$	$1,5 \times 10^{-11}/\text{m}\cdot\text{s}^{-2}$	$1,2 \times 10^{-11}/\text{m}\cdot\text{s}^{-2}$
$y$	$8,7 \times 10^{-12}/\text{m}\cdot\text{s}^{-2}$	$7,7 \times 10^{-12}/\text{m}\cdot\text{s}^{-2}$
$z$	$1,1 \times 10^{-10}/\text{m}\cdot\text{s}^{-2}$	$1,9 \times 10^{-10}/\text{m}\cdot\text{s}^{-2}$

We estimate  $k_{x,y,z}$  by applying a sinusoidal modulation to the active isolation platform along direction  $i$  and measuring simultaneously the acceleration noise spectrum  $S_{a_i}$  and the ultrastable laser phase noise  $S_{\phi}$ . From measurements performed using accelerations of  $10^{-4} \text{ m}\cdot\text{s}^{-2}$  at 2 and 6 Hz, we deduce the acceleration sensitivities listed in Table 1.

These sensitivities are much higher than in our predictions. In particular, the sensitivity along the vertical axis is surprisingly high. In a quiet environment with a white acceleration noise of  $-95 \text{ dB}(\text{m}\cdot\text{s}^{-2})^2/\text{Hz}$ , the vibration-noise contribution to the cavity fractional frequency instability would reach  $1.4 \times 10^{-15}$ , close to the thermal noise limit. In a noisier environment, the vibrations would become a dominant contribution to the cavity frequency noise. Further investigation is needed to determine the origin of this high sensitivity. In particular, the absence of an optical isolator in the free-space optical path implies that etalons might appear and cause extrasensitivity to acoustic noise. In a next study, we will try and eliminate these etalons by inserting an optical isolator in the free-space optical setup.

### B. Thermal Expansion Coefficient of the Cavity

As mentioned in Section 3.A, the cavity was designed to exhibit a CTE turnover point at  $11^\circ\text{C}$ . However, we found no inversion temperature when scanning the cavity setpoint between  $8^\circ\text{C}$  and  $16^\circ\text{C}$ . The cavity shows linear sensitivity instead, with a relative thermal sensitivity of about  $5 \times 10^{-8}/\text{K}$  at  $10^\circ\text{C}$ . This sensitivity might stem from the influence of the stainless-steel holder and the underestimated stiffness of the Viton balls. When designing our cavity, the influence of the holder was indeed not taken into account when calculating the CTE zero-crossing.

This thermal sensitivity yields short-term fluctuations not far below the thermal noise limit of the cavity, which we estimated at about  $1 \times 10^{-15}$ . Indeed, having measured the cavity response to a temperature step as well as the temperature temporal fluctuations at the copper shield, the resulting influence of thermal fluctuations to the fractional frequency instability is expected to scale as  $8.8 \times 10^{-16}\tau$  from 1 to 1000 s. A future upgrade of the setup will include an Invar holder, which should allow us to recover a zero-CTE operating point and reach the cavity thermal noise.

### C. Laser Phase Noise and Fractional Frequency Instability

The stabilized laser phase noise and fractional frequency stability are measured by comparison with a telecom laser stabilized to a spherical cavity. This laser has been characterized independently by comparison with a cryogenic sapphire oscillator in the microwave domain, using optical frequency division techniques [6]. Its frequency stability is better than that of the compact cavity under test.

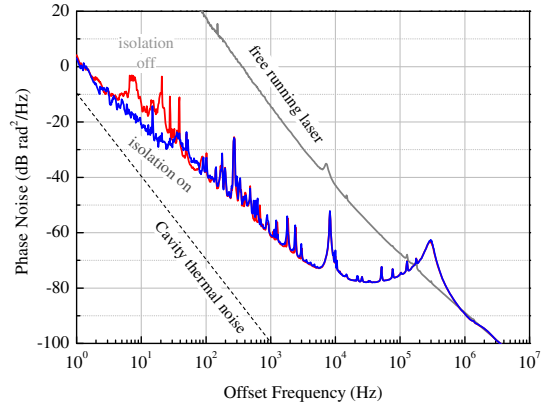


**Fig. 4.** Phase noise of the laser locked to the compact cavity with (blue) and without (red) active vibration isolation, at 194 THz. We display the free-running laser noise (gray curve) and the cavity thermal noise limit (dashed line) for reference.

We measure a phase noise of  $3 \text{ dB rad}^2/\text{Hz}$  at 1 Hz with a slope in  $f^{-2}$  (see Fig. 4). We can see the influence of the active vibration isolation platform between  $\sim 4 \text{ Hz}$  and  $\sim 60 \text{ Hz}$ ; at 1 Hz, the phase noise is not impacted by the residual vibrations of the optical table. Assuming perfect frequency division to 10 GHz, the resulting phase noise would amount to  $-84 \text{ dB rad}^2 \cdot \text{Hz}^{-1}$ .

The phase noise measured at 1 Hz is 13 dB higher than the thermal noise of the cavity. Moreover, the  $f^{-2}$  slope between 3 Hz and 3 kHz denotes white frequency noise. We think that this noise might stem from our electronic frequency-control loop, and we are currently investigating the problem; lower electronic noise combined to higher servo gain should allow us to reach the cavity thermal noise in our current operating conditions.

The measured fractional frequency stability scales as  $7.5 \times 10^{-15}\tau^{1/2}$  at short times, followed by a  $2 \times 10^{-15}\tau$  behavior for  $\tau > 10 \text{ s}$  (Fig. 5). This behavior is compatible with thermal fluctuations. It is in good qualitative agreement with our estimation based on temperature fluctuation measurements and might stem from the high thermal sensitivity of our cavity,

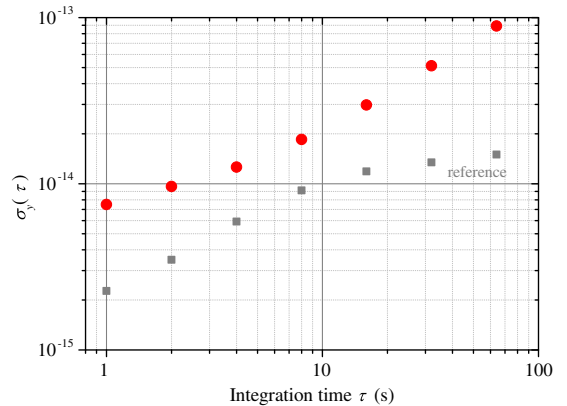


**Fig. 5.** Allan deviation of the laser stabilized onto the ultracompact cavity (red circles). Gray squares represent the Allan deviation of our reference laser stabilized on a spherical ULE cavity [6].

especially for the long-time drift. This will be fixed by the use of an Invar cavity holder with lower temperature sensitivity. The fractional frequency instability measured at 1 s is consistent with the fractional frequency stability computed from the phase noise measured at 1 Hz ( $5 \times 10^{-15}$ ).

These performances are at the state-of-the art for such a short cavity. Our measured fractional frequency instability is comparable with that obtained by Davila-Rodriguez *et al.* at 1 s [9]. Moreover, our simple design results in a setup with a reduced footprint and an overall volume of 30 L, which is interesting for field applications. It is, to our knowledge, the second smallest, with [13] presenting a volume of 24 L.

#### 4. CONCLUSION

In conclusion, we have developed and characterized a 25 mm long pyramidal Fabry–Perot cavity with a ULE spacer, fused silica mirror substrates, and crystalline mirror coatings. Thermal shields and regulations reject the influence of external temperature fluctuations just below  $10^{-15}$ . The acceleration sensitivity of the laser reaches  $2 \times 10^{-10} \text{ m}\cdot\text{s}^{-2}$  along the vertical axis. Even though this is compatible with the low  $10^{-15}$  range when operating in a quiet laboratory environment, this sensitivity must be reduced in order to reach the cavity thermal noise limit in a noisier environment.

The cavity is equipped with highly reflective crystalline coatings and exhibits the highest reported finesse (247,000) to this date using such coatings in an ultrastable laser setup. Our ultrastable laser fits in a volume of 30 L (excluding electronics) and reaches a fractional frequency instability of  $7.5 \times 10^{-15}$  at 1 s. Future upgrades will include a redesigned Invar holder, for better rejection of both temperature and acceleration fluctuations, in order to reach the thermal noise floor around  $1 \times 10^{-15}$ .

**Funding.** Agence Nationale de la Recherche (ANR) (ANR-10-LABX-48-01, ANR-11-EQPX-0033); Centre National d’Études Spatiales (CNES), Région Bourgogne Franche-Comté.

**Acknowledgment.** The authors would like to thank G. D. Cole for the cavity finesse measurement. This work was supported by the LABEX Cluster of Excellence FIRST-TF and by the EQUIPEX OSCILLATOR-IMP, within the Program “Investissements d’Avenir” operated by the French National Research Agency (ANR), by the Council of the Région de

Franche-Comté, and by the Centre National d’Études Spatiales (CNES).

#### REFERENCES

1. A. D. Ludlow, M. M. Boyd, J. Ye, E. Peik, and P. O. Schmidt, “Optical atomic clocks,” *Rev. Mod. Phys.* **87**, 637–701 (2015).
2. T. Kessler, C. Hagemann, C. Grebing, T. Legero, U. Sterr, F. Riehle, M. J. Martin, L. Chen, and J. Ye, “A sub-40-mHz-linewidth laser based on a silicon single-crystal optical cavity,” *Nat. Photonics* **6**, 687–692 (2012).
3. S. Hafner, S. Falke, C. Grebing, S. Vogt, T. Legero, M. Merimaa, C. Lisdat, and U. Sterr, “ $8 \times 10^{-17}$  fractional laser frequency instability with a long room-temperature cavity,” *Opt. Lett.* **40**, 2112–2115 (2015).
4. W. Zhang, M. J. Martin, C. Benko, J. L. Hall, J. Ye, C. Hagemann, T. Legero, U. Sterr, F. Riehle, G. D. Cole, and M. Aspelmeyer, “Reduction of residual amplitude modulation to  $1 \times 10^{-6}$  for frequency modulation and laser stabilization,” *Opt. Lett.* **39**, 1980–1983 (2014).
5. T. M. Fortier, M. S. Kirchner, F. Quinlan, J. Taylor, J. C. Bergquist, T. Rosenband, N. Lemke, A. Ludlow, Y. Jiang, C. W. Oates, and S. A. Diddams, “Generation of ultrastable microwaves via optical frequency division,” *Nat. Photonics* **5**, 425–429 (2011).
6. A. Didier, J. Millo, S. Grop, B. Dubois, E. Bigler, E. Rubiola, C. Lacroûte, and Y. Kersalé, “Ultra-low phase noise all-optical microwave generation setup based on commercial devices,” *Appl. Opt.* **54**, 3682–3686 (2015).
7. X. Xie, R. Bouchand, D. Nicolodi, M. Giunta, W. Hänsel, M. Lezius, A. Joshi, S. Datta, C. Alexandre, M. Lours, P.-A. Tremblin, G. Santarelli, R. Holzwarth, and Y. Le Coq, “Photonic microwave signals with zeptosecond-level absolute timing noise,” *Nat. Photonics* **11**, 44–47 (2016).
8. R. Bouchand, D. Nicolodi, X. Xie, C. Alexandre, and Y. Le Coq, “Accurate control of optoelectronic amplitude to phase noise conversion in photodetection of ultra-fast optical pulses,” *Opt. Express* **25**, 12268–12281 (2017).
9. J. Davila-Rodriguez, F. N. Baynes, A. D. Ludlow, T. M. Fortier, H. Leopardi, S. A. Diddams, and F. Quinlan, “Compact, thermal-noise limited reference cavity for ultra-low-noise microwave generation,” *Opt. Lett.* **42**, 1277–1280 (2017).
10. A. Didier, J. Millo, C. Lacroûte, M. Ouisse, J. Delporte, V. Giordano, E. Rubiola, and Y. Kersalé, “Design of an ultra-compact reference ULE cavity,” *J. Phys.* **723**, 012029 (2016).
11. T. Legero, T. Kessler, and U. Sterr, “Tuning the thermal expansion properties of optical reference cavities with fused silica mirrors,” *J. Opt. Soc. Am. B* **27**, 914–919 (2010).
12. G. D. Cole, W. Zhang, M. J. Martin, J. Ye, and M. Aspelmeyer, “Tenfold reduction of Brownian noise in high-reflectivity optical coatings,” *Nat. Photonics* **7**, 644–650 (2013).
13. Q. F. Chen, A. Nevsky, M. Cardace, S. Schiller, T. Legero, S. Häfner, A. Uhde, and U. Sterr, “A compact, robust, and transportable ultrastable laser with a fractional frequency instability of  $1 \times 10^{-15}$ ,” *Rev. Sci. Instrum.* **85**, 113107 (2014).